X-ray diffraction peaks at glancing incidence and glancing exit from highly mismatched epitaxial layers

V. M. Kaganer[a)]
Paul-Drude-Institut für Festkörperelektronik, Hausvogteiplatz 5-7, 10117 Berlin, Germany

A. Shalimov and J. Bak-Misiuk
Institute of Physics, Polish Academy of Sciences, Aleja Lotników 32/46, 02-668 Warsaw, Poland

K. H. Ploog
Paul-Drude-Institut für Festkörperelektronik, Hausvogteiplatz 5-7, 10117 Berlin, Germany

(Received 2 March 2006; accepted 10 June 2006; published online 14 July 2006)

We find that the widths of double-crystal x-ray diffraction peaks in asymmetric reflections of relaxed GaAs/Si(001) heteroepitaxial layers in reciprocal diffraction geometries (glancing incidence and glancing exit) are notably different. This observation is in agreement with previous measurements on other heteroepitaxial systems but apparently contradicts the reciprocity principle of electrodynamics. We show that the apparent contradiction originates from the summation of the scattered waves that are collected by the detector in a double-crystal setup and resolve it by giving an appropriate description of the peak widths. © *2006 American Institute of Physics*.
[DOI: 10.1063/1.2221885]

X-ray diffraction is a versatile tool to study the strain state of crystalline objects. The mean strain is obtained from positions of the diffraction peaks and the strain variations (microstrain) from widths and shapes of the peaks. In most cases, the kinematical theory of x-ray diffraction can be applied.[1–3] It states that the x-ray scattering intensity depends only on the momentum transfer $\mathbf{k}_f - \mathbf{k}_i$, where $\mathbf{k}_i$ and $\mathbf{k}_f$ are the wave vectors of the incident and diffracted waves, respectively. We do not consider in this letter the exceptional case when $\mathbf{k}_i$ or $\mathbf{k}_f$ make a small angle to the surface, comparable with the angle of total external reflection.[3,4] In that case, the diffracted intensity depends on the angles to the surface and cannot be considered as a function of the momentum transfer alone.

In this letter, we analyze x-ray diffraction measurements of the highly mismatched heteroepitaxial system GaAs/Si(001). We find that the widths of the double-crystal rocking curves from asymmetric reflections in two reciprocal geometries, with the incidence angle smaller than the exit angle [glancing incidence diffraction (GID)] and with the exit angle smaller than the incidence angle [glancing exit diffraction (GED)], are notably different. Similar experimental results were obtained earlier on other highly mismatched heterostructures, such as GaAs/InAs and InAs/GaAs.[5] These observations apparently contradict the main statement of kinematical theory that the diffracted intensity depends on the momentum transfer $\mathbf{k}_f - \mathbf{k}_i$, rather than $\mathbf{k}_i$ and $\mathbf{k}_f$ separately. The application of kinematical theory is justified, since the incident and the exit angles are much larger than the critical angle of total external reflection, and the measured peak widths are much larger than the dynamical rocking curve width.

These observations also apparently contradict a more fundamental statement, the reciprocity principle of electrodynamics,[6,7] which states that the intensity does not change if the source and the observation point are interchanged. Reciprocity is often used in practice to solve diffraction problems.[3,4] Therefore, the resolution of the apparent contradiction has not only fundamental but also practical impact.

The present work is devoted to a detailed comparison of the GID and GED measurements. The study was performed on 2 μm thick GaAs epitaxial layers grown by molecular beam epitaxy on vicinal Si(001).[8] The x-ray measurements were carried out with a high-resolution x-ray diffractometer Philips X'Pert using a four bounce asymmetric Ge(220) monochromator and Cu $K\alpha$ radiation. The triple-crystal measurements were performed with a three bounce Ge(220) analyzer. We have studied a series of samples with miscut directions [110] and $[1\bar{1}0]$ and miscut angles varying from 0.5° to 7.5°. The diffraction measurements performed both along and perpendicular to the miscut direction do not reveal any dependence of the measured curves on the miscut angle or orientation. The GaAs films are fully relaxed. Transmission electron microscopy shows that, after rapid thermal annealing of the samples, the majority of the misfit dislocations are edge dislocations that form a regular network.[8,9] These periodic dislocations cause nonuniform strain only in a very thin (thinner than the mean distance between dislocations of 9 nm) layer at the interface[10] and do not contribute to the x-ray peak broadening studied in the present work. The observed peak broadening is due to the remaining 60° dislocations randomly distributed at the interface.

Figure 1 compares the full widths at half maximum (FWHMs) of the double-crystal rocking curves measured in different reflections. The asymmetric reflections are measured in GID and GED geometries. The peak widths are distinctly different, up to a factor of 3 in the 444 reflection, and agree with similar observations on GaAs/InAs and InAs/GaAs heteroepitaxial films.[5] The plot of the square of FWHM vs $\tan^2\theta$ in Fig. 1 is the Williamson-Hall plot,[11,12] which is expected to be linear with a slope giving the strain effect. The plot in Fig. 1 is far from being linear and, moreover, shows notably different FWHMs in the GID and GED

a)Electronic mail: kaganer@pdi-berlin.de

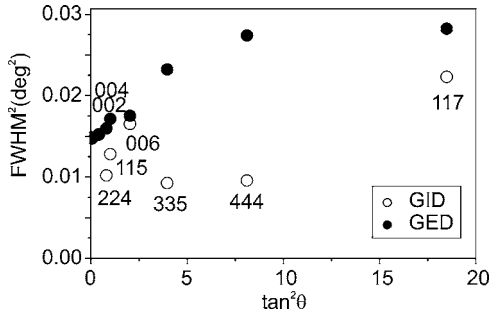

FIG. 1. Williamson-Hall plot for relaxed GaAs layer on Si(001). Open and full circles correspond to GID and GED geometries, respectively.

geometries. This latter result is in apparent contradiction to the reciprocity principle. Let us therefore investigate it in more detail.

The largest difference between the FWHMs in the GID and GED geometries is revealed in the most asymmetric 444 reflection. Figure 2(a) presents the corresponding peak profiles. They are measured in the double-crystal diffraction geometry with a detector acceptance of 1°. Figure 2(b) shows, for comparison, the triple-crystal peaks. The GID and GED profiles coincide in both ω and ω-2θ scans, as required by the reciprocity principle. We conclude that the difference in the peak widths in the two geometries in Fig. 2(a) originates from the summation of the intensities of all diffracted beams that are within the detector acceptance range in the double-crystal diffraction.

This explanation is justified further by comparing the reciprocal space maps measured in the 444 reflection in GID and GED geometries, Fig. 3. The GED measurements were performed after a 180° rotation of the sample, so that the two maps are mirror images, as required by the reciprocity principle. The intensity distributions are of elliptical shape with the main axis close to, but not coinciding with, the normal to the reciprocal lattice vector **Q**. Such rotations of the intensity distributions have been observed and discussed previously.[13] The source of the diffuse scattering, namely, the misfit dislocations, is distributed at the heteroepitaxial interface parallel to the surface, and there is no symmetry constraint that would require the intensity distribution in an asymmetric reflection to extend exactly along **Q** or its normal. When a double-crystal rocking curve is measured, the diffracted waves of different directions are integrated by the detector. The wave vectors of all diffracted waves lie on the Ewald sphere, as required by momentum conservation in elastic x-ray diffraction. A relevant piece of the sphere can be replaced by the plane normal to the diffracted beam, as shown in Fig. 3 by broken lines. Rotation of the sample during the double-crystal rocking curve measurement corresponds to

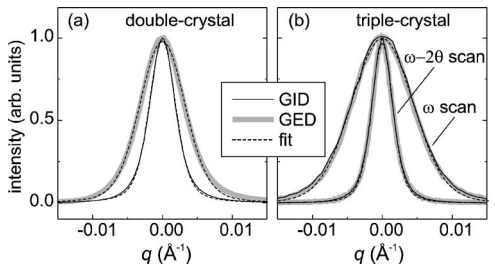

FIG. 2. Profiles of the 444 diffraction peaks in double-crystal (a) and triple-crystal (b) diffraction experiments.

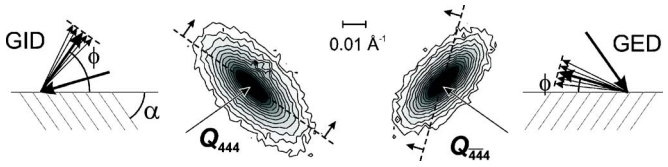

FIG. 3. Schemes of the GID and GED measurements and the reciprocal space maps in the two diffraction geometries. The broken lines perpendicular to the respective diffracted beam direction show the integration performed during a double-crystal measurement.

the movement of the Ewald sphere through the diffraction spot, as shown by arrows in Fig. 3.

The Ewald sphere in the two reciprocal geometries is differently oriented with respect to the main axes of the intensity distributions. It is evident from a comparison of Figs. 3(a) and 3(b) that, during sample rotation, the diffraction spot passes through the Ewald sphere faster in the GID geometry, resulting in a narrower peak. That explains the difference between the GID and GED peak widths in Figs. 1 and 2(a) and resolves the apparent contradiction with the reciprocity principle. Thus, the integration of the diffracted waves by the detector is of primary importance for the peak profile analysis.

A detailed theoretical analysis of the diffraction peak profiles from misfit dislocations was performed in Ref. 13. In the case of large dislocation densities, which are of interests here, the calculation of the diffracted intensity involves only correlations between pairs of closely spaced points. Their separations x along the surface and ζ normal to it are small compared to the layer thickness d. The translational symmetry is broken in the surface normal direction, so that the correlation function depends not only on the separation (x,ζ) between the two points but also on their depth z in the film. Then, the diffracted intensity can be written as

$$I(q_x,q_z)=\int\int_{-\infty}^{\infty}dxd\zeta\int_0^d dz e^{iq_x x+iq_z\zeta}e^{-T(x,\zeta,z)}. \tag{1}$$

The exponent of the correlation function $T(x,\zeta,z)$ can be represented as[13] $T(x,\zeta,z)=w_{xx}(z)x^2+2w_{xz}(z)x\zeta+w_{zz}(z)\zeta^2$, where the expressions for the functions $w_{ij}(z)$ (here $i,j=x,z$) are given in Ref. 13. The broken lines in Fig. 2(b) are the fits of the respective scans to Eq. (1).

The intensity distribution of the double-crystal measurement can be obtained by integrating Eq. (1) over the plane tangential to the direction of the diffracted beam. Denoting by ϕ the angle that the diffracted beam makes with the surface, see Fig. 3, proceeding to the wave vector components q along the diffracted beam $\mathbf{k}_f$ and $q_\perp$ normal to it, and integrating Eq. (1) over $q_\perp$, we obtain

$$\mathcal{I}(q)=\int_0^d\frac{dz}{w}\exp(-q^2/4w), \tag{2}$$

where $w=w_{xx}\cos^2\phi+2w_{xz}\sin\phi\cos\phi+w_{zz}\cos^2\phi$. The integration over the Ewald sphere for the double-crystal experiments leads to simplifications similar to the powder diffraction case.[14] The angle ϕ is equal to $\phi=\alpha+\theta$ for GID and $\phi=\pi-(\alpha-\theta)$ for GED. Here α is the angle between scattering planes and the surface, Fig. 3, and θ is the Bragg angle. The difference between the ϕ values in the two reciprocal geometries gives rise to a difference in the peak widths. The

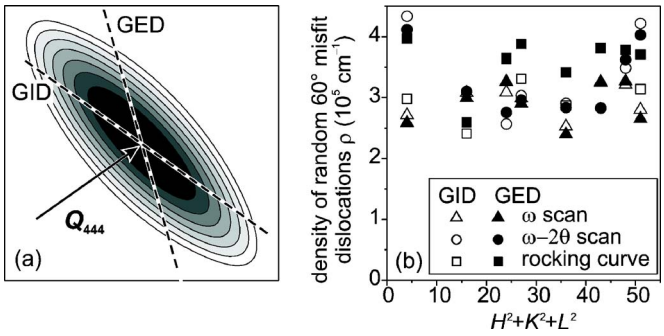

FIG. 4. Calculated reciprocal space map in reflection 444 (a) and the linear density ρ of random 60° misfit dislocations obtained by fits from different types of measurements for different reflections *HKL* (b).

broken lines in Fig. 2(a) are the fits of the measured peak profiles to Eq. (2).

Figure 4(a) presents a calculated reciprocal space map for the same conditions as the measured maps in Fig. 3. The intensity distribution is of elliptical shape and elongated in the same direction as the experimental one, not coinciding with the normal to **Q**. The broken lines are the integration directions for GID and GED geometries. The asymmetry between the two geometries is evident.

The calculated peak profiles fit the measured ones using just one parameter, namely, the dislocation density. An example of the fits for the 444 reflection is shown in Fig. 2 by the broken lines. Figure 4(b) presents the fit results for different reflections, scans, and geometries. The mean linear dislocation density obtained in the fits is $\rho=(3.2\pm0.5)\times10^5$ cm^{-1}, much smaller than the total misfit dislocation density required to release the mismatch between the film and the substrate. If the remaining mismatch is released by periodic edge dislocations,[8,9] the fraction of random 60° dislocations is 26% of the total misfit dislocation density. Here we take into account that the Burgers vector component in the interfacial plane is two times larger for edge dislocations. This fraction is larger than the fraction of 60° dislocations obtained by transmission electron microscopy (TEM).[9] Our study of FWHMs of the x-ray diffraction peaks on a series of the GaAs/Si(001) samples, to be presented elsewhere, shows that the fraction of 60° dislocations varies in different samples from 9% to 26%, in an agreement with the TEM results.

In summary, we find that different peak widths in GID and GED geometries are observed only in double-crystal rocking curves, while triple-crystal scans in the reciprocal geometries give coincident diffraction curves. The difference of the double-crystal curves is explained by the summation of the scattered waves that are accepted by the detector.

The authors thank A. Georgakilas for sample preparation and M. Calamiotou for useful discussions. This work was partially supported by European Community program G1MA-CT-2002-4017 (Centre of Excellence CEPHEUS) and by the Polish Committee for Scientific Research under Grant No. P03B11528.

[1] B. E. Warren, *X-Ray Diffraction* (Addison-Wesley, Reading, MA, 1969).
[2] M. A. Krivoglaz, *X-Ray and Neutron Diffraction in Nonideal Crystals* (Springer, Berlin, 1996).
[3] U. Pietsch, V. Holý, and T. Baumbach, *High-Resolution X-Ray Scattering: From Thin Films to Lateral Nanostructures* (Springer, Berlin, 2004).
[4] S. K. Sinha, E. B. Sirota, S. Garoff, and H. B. Stanley, Phys. Rev. B **38**, 2297 (1988).
[5] C. Ferrari, L. Francesio, P. Franzosi, and S. Gennari, Appl. Phys. Lett. **69**, 4233 (1996).
[6] M. von Laue, *Röntgenstrahl-Interferenzen* (Akademische, Leipzig, 1948).
[7] L. D. Landau and E. M. Lifshitz, *Electrodynamics of Continuous Media* (Pergamon, London, UK, 1960).
[8] A. Georgakilas, P. Panayotatos, J. Stoemenos, J.-L. Mourrain, and A. Christou, J. Appl. Phys. **71**, 2679 (1992).
[9] A. Georgakilas and A. Christou, J. Appl. Phys. **76**, 7332 (1994).
[10] D. K. Satapathy, V. M. Kaganer, B. Jenichen, W. Braun, L. Däweritz, and K. H. Ploog, Phys. Rev. B **72**, 155303 (2005).
[11] G. K. Williamson and W. H. Hall, Acta Metall. **1**, 22 (1953).
[12] J. E. Ayers, J. Cryst. Growth **135**, 71 (1994).
[13] V. M. Kaganer, R. Köhler, M. Schmidbauer, R. Opitz, and B. Jenichen, Phys. Rev. B **55**, 1793 (1997).
[14] V. M. Kaganer, O. Brandt, A. Trampert, and K. H. Ploog, Phys. Rev. B **72**, 045423 (2005).